

Published in final edited form as:

*Nature*. 2008 October 2; 455(7213): 689–692. doi:10.1038/nature07215.

## CDK targets Sae2 to control DNA-end resection and homologous recombination

Pablo Huertas<sup>1</sup>, Felipe Cortés-Ledesma<sup>2</sup>, Alessandro A. Sartori<sup>1,†</sup>, Andrés Aguilera<sup>2</sup>, and Stephen P. Jackson<sup>1</sup>

<sup>1</sup>The Wellcome Trust and Cancer Research UK Gurdon Institute, and Department of Zoology, University of Cambridge, Tennis Court Road, Cambridge CB2 1QN, UK.

<sup>2</sup>Centro Andaluz de Biología Molecular y Medicina Regenerativa CABIMER, Universidad de Sevilla-CSIC, Avenida Américo Vespucio s/n, 41092 Sevilla, Spain.

### Abstract

DNA double-strand breaks (DSBs) are repaired by two principal mechanisms: non-homologous end-joining (NHEJ) and homologous recombination (HR)<sup>1</sup>. HR is the most accurate DSB repair mechanism but is generally restricted to the S and G2 phases of the cell cycle, when DNA has been replicated and a sister chromatid is available as a repair template<sup>2–5</sup>. By contrast, NHEJ operates throughout the cell cycle but assumes most importance in G1 (refs 4, 6). The choice between repair pathways is governed by cyclin-dependent protein kinases (CDKs)<sup>2,3,5,7</sup>, with a major site of control being at the level of DSB resection, an event that is necessary for HR but not NHEJ, and which takes place most effectively in S and G2 (refs 2, 5). Here we establish that cell-cycle control of DSB resection in *Saccharomyces cerevisiae* results from the phosphorylation by CDK of an evolutionarily conserved motif in the Sae2 protein. We show that mutating Ser 267 of Sae2 to a non-phosphorylatable residue causes phenotypes comparable to those of a *sae2Δ* null mutant, including hypersensitivity to camptothecin, defective sporulation, reduced hairpin-induced recombination, severely impaired DNA-end processing and faulty assembly and disassembly of HR factors. Furthermore, a Sae2 mutation that mimics constitutive Ser 267 phosphorylation complements these phenotypes and overcomes the necessity of CDK activity for DSB resection. The Sae2 mutations also cause cell-cycle-stage specific hypersensitivity to DNA damage and affect the balance between HR and NHEJ. These findings therefore provide a mechanistic basis for cell-cycle control of DSB repair and highlight the importance of regulating DSB resection.

To initiate HR, one strand of the broken DNA duplex is resected in the 5'→3' direction, generating single-stranded DNA (ssDNA) that can anneal with a homologous DNA duplex<sup>8</sup>. In *S. cerevisiae*, effective resection and HR require sustained Cdc28/C1b (Cdk1/cyclin B) kinase activity<sup>2,3,5</sup>, although the CDK targets mediating this control are still unknown. One potential target is Sae2, a protein first identified as being required for meiotic recombination. Sae2 controls the initiation of DNA-end resection in meiotic and mitotic cells<sup>9–12</sup> and was recently shown to be a DNA endonuclease<sup>13</sup>. Previous work has shown that Sae2 is targeted by the Mec1 and Tel1 kinases in response to DNA damage, generating forms of Sae2 with

**Author Information** Reprints and permissions information is available at [www.nature.com/reprints](http://www.nature.com/reprints). Correspondence and requests for materials should be addressed to S.P.J. ([s.jackson@gurdon.cam.ac.uk](mailto:s.jackson@gurdon.cam.ac.uk)).

<sup>†</sup>Present address: Institute of Molecular Cancer Research, University of Zurich-Irchel, Winterthurerstrasse 190, CH-8057 Zurich, Switzerland.

#### Author Contributions

A.A.S. identified the homology between Sae2 and CtIP, cloned *SAE2* into pGEX-4T1 and made the original *sae2-S267A* and *sae2-S267E* mutations. All the experiments shown were performed by P.H. and were conceived by P.H. and S.P.J., except those on SCR analyses that were performed by F.C.-L. and conceived by F.C.-L. and A.A. P.H. and S.P.J. wrote the paper. All authors discussed and commented on the manuscript.

decreased mobility in SDS-polyacrylamide gels<sup>14</sup>. Such alterations in Sae2 gel-mobility also occurred in unperturbed cycling cells, specifically in S and G<sub>2</sub>, indicating that Sae2 might be a Cdc28 target (data not shown, Fig. 2b and Supplementary Fig. 2a). In accord with this idea, the amount of slower-migrating Sae2 was diminished when Cdc28 was inactivated in G<sub>2</sub>-synchronized cultures by galactose-driven expression of the Cdc28/C1b repressor, Sic1 (ref. 15) (Fig. 1a).

Sae2 contains three potential CDK phosphorylation sites (Fig. 1b and Supplementary Fig. 1); two of these—Ser 267 and Ser 134—received the highest scores for predicted phosphorylation sites in the protein (Supplementary Table 1). Ser 267 maps to the Sae2 region most highly conserved with its non-yeast orthologues (Fig. 1b), which include human CtIP, *Caenorhabditis elegans* Com1 and *Arabidopsis thaliana* Com1 (refs 16–18). To address the possible function(s) of Ser 267 and other potential target sites for CDK in Sae2, we generated yeast strains in which each site was individually mutated to a non-phosphorylatable alanine residue. The *sae2-S267A* mutant showed strong hypersensitivity towards the topoisomerase I inhibitor camptothecin (Fig. 1c and Supplementary Fig. 2b; Supplementary Fig. 2c shows that this mutant is nearly as sensitive as the *sae2Δ* strain). By contrast, *sae2-S134A*, *sae2-S179A* and *sae2-S134A,S179A* cells did not show detectable hypersensitivity to camptothecin, and combining *sae2-S267A* with these other mutations showed no synergistic effect (Supplementary Fig. 2b). When we mutated Ser 267 to glutamic acid to mimic constitutive phosphorylation, the resulting strain displayed no detectable hypersensitivity to camptothecin (Fig. 1c and Supplementary Fig. 2c). Together with the fact that mutation of Ser 267 did not alter Sae2 protein expression (Fig. 1d), these data suggested that Ser 267 phosphorylation is required for Sae2 function. Furthermore, as the major cytotoxic lesions for camptothecin are DSBs arising when replication forks encounter trapped topoisomerase I–DNA complexes<sup>19</sup>, these results suggested that phosphorylation of Sae2 on Ser 267 is important for responses to DSBs generated during S phase. Indeed, the *sae2*-null and *sae2-S267A* strains, but not the *sae2-S267E* strain, showed hypersensitivity to methyl methanesulphonate (MMS), which also yields DSBs in S phase (Supplementary Fig. 2d). Consistent with analogous residues controlling the activity of Sae2-related proteins in other species, human U2OS cells downregulated for endogenous CtIP and expressing short interfering RNA (siRNA)-resistant *GFP-CtIP-T847A* were as sensitive to camptothecin as control cells expressing *GFP* (green fluorescent protein) alone, whereas cells expressing a phospho-mimicking CtIP derivative (*GFP-CtIP-T847E*) showed higher resistance to camptothecin (Fig. 1e; for expression levels and downregulation see Supplementary Fig. 2e).

Efficient phosphorylation of CDK substrates *in vivo* often requires the binding of cyclin to an Arg-X-Leu (RXL) motif in the target<sup>20</sup>. Such a motif is present upstream of Ser 267 in Sae2 (Fig. 1b and Supplementary Fig. 1), and mutating this motif (*Sae2-R223A,L225A*) caused hypersensitivity to camptothecin as severe as that of *sae2-S267A* or *sae2Δ* cells (Fig. 1c) even though the mutated proteins were expressed at normal levels (Fig. 1d). Furthermore, the camptothecin hypersensitivity caused by the *Sae2-R223A,L225A* mutation was largely suppressed when the protein also contained the phospho-mimicking Sae2 S267E mutation (Fig. 1c). Collectively, these findings strongly suggested that Sae2 function requires its modification by CDK–cyclin complexes.

To examine the phosphorylation of Sae2 on Ser 267 directly, we raised a phosphospecific antibody against this site ( $\gamma$ S267). Western immunoblotting revealed that this antibody specifically detected immunoprecipitated wild-type Sae2 but not the *Sae2-S267A* or *Sae2-R223A,L225A* proteins (Fig. 2a). Furthermore, the antibody detected the slower-migrating form of Sae2 that was present at elevated levels in G<sub>2</sub>-synchronized cultures (Fig. 2b), indicating that phosphorylation of Sae2 on Ser 267 is subject to cell-cycle control. Notably,

Sae2 immunoprecipitation recovered cyclins Clb3 and Clb2 from extracts prepared from G2-synchronized cells but not from G1 cells (Fig. 2b). Also consistent with Sae2 being a direct target of CDK, incubation of purified glutathione *S*-transferase-fused Sae2 protein—but not the S267A mutant—with recombinant CDK-cyclin complexes and ATP produced Ser 267 phosphorylation (Fig. 2c).

Further analyses suggested that all aspects of Sae2 function require phosphorylation at Ser 267. Thus, like *sae2Δ* cells, *sae2-S267A* cells were severely compromised in hairpin-induced recombination<sup>21</sup>, whereas *sae2-S267E* cells behaved similarly to the wild-type (Fig. 2d). Furthermore, whereas homozygous diploid *sae2-S267E* cells produced viable spores at levels similar to those produced by the wild-type strain, like *sae2Δ* cells<sup>10,12</sup>, the *sae2-S267A* homozygous mutant strain showed a severe sporulation defect and almost no spore viability (Figs 2e and 2f). A defect in spore viability due to mutations in Ser 267 or Pro 268 has also been reported recently<sup>18</sup>.

Sae2 regulates resection of chromosomal DSBs formed by the HO endonuclease<sup>9</sup>. To determine whether Sae2 Ser 267 controls this function, we generated an irreparable HO-induced DSB in the *MAT* locus and analysed resulting samples with a neutral dot-blot approach that detected only resected DNA<sup>22</sup>. For this we used three probes: one directly adjacent to the HO cleavage site, one 5 kilobases (kb) downstream and one at the *LEU2* locus, about 100 kb distal from the HO site, as a negative control. Significantly, *sae2Δ* cells and cells bearing the *sae2-S267A* mutation were impaired in resection close to the HO site, and this impairment was even more pronounced when assayed 5 kb away (Fig. 3a). By contrast, the *sae2-S267E* mutant carried out resection almost as efficiently as the wild-type strain (Fig. 3a and Supplementary Fig. 3a).

To test whether Cdc28/Cdk1-mediated Sae2 phosphorylation promotes DSB resection, we assessed resection in a strain expressing a Cdc28 derivative (*cdc28-as1*) that can be specifically inhibited by the ATP analogue 1NM-PP1 (ref. 23). Whereas inhibition of Cdk1 markedly curtailed end resection in a strain expressing wild-type Sae2, it had little effect in the *sae2-S267E* mutant when resection was measured close to the HO site (Fig. 3b and Supplementary Fig. 3b). Nevertheless, the inhibitor still had some effect on the *sae2-S267E* strain when resection was assessed at the 5 kb distal site (Fig. 3b and Supplementary Fig. 3b). We therefore conclude that phosphorylation of Sae2 on Ser 267 by Cdc28/Cdk1 is required for effective DSB resection but that additional Cdk1 target sites are required for resection to take place optimally. One candidate for such an additional CDK target is Rad9, which is phosphorylated by Cdc28 and was recently shown to affect DSB resection<sup>24</sup>.

*S. cerevisiae* Mre11 is recruited quickly to DSB sites, then replaced by the HR protein Rad52 as ssDNA is formed in S and G2 cells<sup>24</sup>. We found that, like *SAE2* deletion<sup>25</sup>, the *sae2-S267A* mutation caused Mre11 foci to persist longer than in wild-type cells (Fig. 4a) and delayed Rad52 focus formation in S/G2 after X-ray treatment (Fig. 4b). In contrast, the *sae2-S267E* mutant displayed Mre11 focus disassembly kinetics similar to the wild-type strain (Fig. 4a), and in fact reproducibly formed Rad52 foci faster in S and G2 than the wild-type strain (Fig. 4b). As expected, essentially no Rad52 foci were detected in wild-type G1 cells, because DSBs are not efficiently resected. By contrast—and unlike the *sae2-S267A* mutant—the *sae2-S267E* mutant formed Rad52 foci in G1 at later time points (Fig. 4c), confirming that DNA ends are processed to some degree in this mutant even in the absence of active CDK (Fig. 3b).

To address the impact of aberrant DSB processing on DSB repair, we irradiated asynchronous, G2-arrested and G1-arrested cell cultures, then kept cells in the same state (asynchronous, G2 or G1) for 6 h to allow DNA repair. Cells were subsequently plated and

colony formation was used to determine survival. When we analysed asynchronous cultures, the *sae2Δ* strain showed moderate hypersensitivity to radiation (as shown previously<sup>26</sup>) and similar, although slightly more pronounced, hypersensitivities were displayed by the *sae2-S267A* and *sae2-S267E* strains (Fig. 4d). Moreover, the two Ser 267 mutations had markedly different effects in G1 and G2 (Fig. 4d). Thus, whereas the *sae2-S267A* strain was more sensitive to radiation than the control strain in G2, little or no G2 hypersensitivity was shown by the *sae2-S267E* strain. In contrast, *sae2-S267E* cells showed marked hypersensitivity to radiation in G1, whereas the *sae2*-null and *sae2-S267A* cells did not.

The above data suggested that the *sae2-S267A* and *sae2*-null strains, but not the *sae2-S267E* strain, are defective in HR because of impaired DSB resection in G2, and also suggested that the hypersensitivity of the *sae2-S267E* mutant to radiation in G1 reflects aberrant DSB resection, thus impairing NHEJ and/or triggering futile attempts to carry out HR in the absence of a sister chromatid. To test these ideas, we determined HR and NHEJ efficiencies in various *sae2* mutant backgrounds. When we used an assay in which HR intermediates were monitored by Southern blot analysis<sup>27</sup>, the *sae2*-null and *sae2-S267A* mutants showed delayed HR, whereas the *sae2-S267E* mutant showed slightly accelerated recombination (Fig. 4e and Supplementary Fig. 4). Furthermore, by measuring NHEJ with an *in vivo* plasmid-recircularization assay<sup>28</sup>, we found that cells lacking Sae2 or bearing the *S267A* mutation had enhanced ( $P < 0.05$  compared with wild-type) NHEJ efficiencies, regardless of whether the DSB contained a 5' overhang, a 3' overhang or a blunt end (Fig. 4f). In addition, and in agreement with an increased propensity for DSB resection that would impair NHEJ, *sae2-S267E* mutant cells showed a decrease in NHEJ efficiency when overhang substrates were used ( $P < 0.05$ ; Fig. 4f). By retrieving repaired plasmids from independent clones and sequencing them, we found that in wild-type cells most repair took place accurately or by micro-homology-mediated end-joining involving pairs of 4-bp repeats separated by 7 or 418 bp to create small or moderate deletions (Fig. 4g). In agreement with less efficient resection taking place in the *sae2*-null and *sae2-S267A* mutant strains, such cells favoured accurate repair or repair involving small (7-bp) deletions ( $P < 10^{-8}$ ; Fig. 4g; similar data were reported for *sae2Δ* cells<sup>29</sup>). In contrast, *sae2-S267E* mutant cells showed little accurate NHEJ and, instead, most repair products contained larger deletions of up to 2 kb ( $P < 10^{-4}$ ; Fig. 4g).

Thus, Cdc28/Cdk1-mediated Sae2 phosphorylation modulates the balance between NHEJ and HR during the cell cycle. These results lend strong support to models in which the commitment to DSB resection is highly regulated to ensure that the cell engages the most appropriate DNA repair pathway, thereby optimizing genome stability. As Sae2 has endonuclease activity<sup>13</sup>, we favour a model in which Sae2, possibly in cooperation with the Mre11-Rad50-Xrs2 (MRX) complex, facilitates resection in S/G2 by mediating an endonucleolytic cleavage close to the DNA break, thus generating a clean end that can serve as an efficient substrate for nucleases such as MRX and Exo1. Sae2 activity might be particularly important to initiate resection at DSBs that contain covalently bound proteins that would otherwise resist exonuclease action; indeed, this would explain why deletion of *SAE2* causes defective removal of Spo11-DNA adducts during meiosis and marked hypersensitivity to camptothecin. Sae2 might also initiate resection at radiation-induced DSBs that are resistant to exonucleases because they bear protein-DNA crosslinks or complex damage to bases at their termini. By contrast, at sites of clean DSBs, *SAE2* deletion would only slow down resection and ensuing HR, thus explaining why *sae2* mutants are not as sensitive to radiation as other HR mutants<sup>22</sup>. Finally, we note that the motif encompassing Ser 267 of Sae2 is highly conserved in Sae2 counterparts in higher eukaryotes, and that mutation of the analogous Thr 847 site in human CtIP to Ala (but not to Glu) yields hypersensitivity to camptothecin. This suggests that analogous CDK-control mechanisms for DSB resection operate in many other organisms. One exception to this, however, is likely to

be provided by *Schizosaccharomyces pombe*, whose Sae2/CtIP homologue, Ctp1, lacks a CDK site analogous to Ser 267 of Sae2. In this case, it seems that, rather than controlling Ctp1 phosphorylation, the CDK machinery instead regulates the protein expression of Ctp1 (ref. 30). Nevertheless, although some species-specific variations undoubtedly exist, we speculate that Sae2/CtIP/Com1/Ctp1 proteins will turn out to have ubiquitous functions in facilitating DSB resection in S and G2 and modulating the choice of DSB repair pathway in eukaryotic cells.

## METHODS SUMMARY

A *sae2Δ* strain in W303 background<sup>9,14</sup> was transformed with plasmids harbouring the indicated *SAE2* mutant and used in all experiments except those listed below. For Figs 1a and 2b, a Sae2-TAP strain (Open Biosystems) was used. In Fig. 2e, f, a strain harbouring the indicated Sae2 mutant at its chromosomal locus in the SK1 background was used. For Fig. 3, we deleted *SAE2* in a strain harbouring the *cdc28as1* allele in the JKM179 background<sup>5</sup>. The W5573-15D strain was used in Fig. 4a-c (ref. 25). A *sae2*-deleted OIS-15 strain was used in Fig. 4e (ref. 27). Yeasts were grown with standard procedures. When indicated, cells were arrested in G1 with  $\alpha$ -factor and in G2 with nocodazole. DNA resection assays<sup>22</sup>, focus formation<sup>25</sup>, recombination between sister chromatids<sup>27</sup> and NHEJ assays<sup>30</sup> were as described previously. CtIP downregulation was as previously reported<sup>17</sup>. Western blotting was by standard methods.

## Supplementary Material

Refer to Web version on PubMed Central for supplementary material.

## Acknowledgments

We thank M. P. Longhese, R. Rothstein, K. Lobachev, M. Lichten and M. Foiani for providing strains, and R. Driscoll, S. Gravel, K. Dry and K. Miller for helpful discussions and comments on the manuscript. P.H. is the recipient of a Long-Term EMBO Fellowship. A.A.S. is supported by a Swiss National Foundation Grant. The S.P.J. laboratory is supported by grants from Cancer Research UK and the European Community (Integrated Project DNA repair, grant LSHG-CT-2005-512113). The A.A. laboratory is supported by grants from the Spanish Ministry of Science and Education (BFU2006-05260 and CDS2007-0015) and Junta de Andalucía (CVI624).

## Appendix

### METHODS

#### TAP-tagged Sae2 immunoprecipitation

TAP complexes were purified by a variation of previously described methods<sup>31</sup>. Cultures (250 ml) of TAP-tagged Sae2 variants were collected by centrifugation at 4 °C and resuspended in 1 volume of 50 mM Tris-HCl pH 7.5, 100 mM NaCl, 1.5 mM MgCl<sub>2</sub>, 0.15% Nonidet P40 in the presence of protease inhibitor (Roche) and phosphatase inhibitors. Extracts were prepared with a One-Shot cell disruptor (Constant Systems) and centrifuged for 1 h at 3,000 r.p.m. (1400 g) and 4 °C. Next, samples were incubated for 2 h at 4 °C with IgG-Sepharose (Amersham) pre-equilibrated in the same buffer. The matrix was then packed in a column and washed with 50 ml of the same buffer at 4 °C. Next, the resin was resuspended in 100  $\mu$ l of 10 mM Tris-HCl pH 8.0, 150 mM NaCl, 0.1% Nonidet P40, 0.5 mM EDTA, 1 mM dithiothreitol, transferred to a microcentrifuge tube, incubated for 2 h at 16 °C and then overnight at 4 °C with 10 U of TEV protease (Qiagen) to release Sae2 complexes from the beads. Through this procedure, Sae2 retained half of the TAP tag that could then be detected with anti-TAP antibody (Open Biosystems). Samples were centrifuged for 1 min at maximum speed (2900 g) at 4 °C; the supernatant was transferred to

a new tube and 100  $\mu$ l of sample loading buffer was added followed by immunoblot analysis by SDS-PAGE with the following antibodies: anti-TAP, anti-  $\gamma$ S267 (custom made; Eurogentec), anti-PGK1 (Molecular Probes), Cdc28, Clb2 and Clb3 (Santa Cruz).

### Human cell survival assays

Human U2OS cells expressing siRNA-resistant wild-type or mutant GFP-CtIP fusions were downregulated for endogenous CtIP with a previously published siRNA<sup>17</sup>, and 72 h afterwards were exposed to doses of camptothecin for 1 h. Survivals represent the number of colonies formed after 12 days normalized with an unirradiated control.

### Sporulation efficiency

Homozygous diploids were grown overnight in YPAD medium, washed twice with warm sporulation medium, left in sporulation medium for 24 h at 30 °C, then fixed with 50% ethanol and stained with 4,6-diamidino-2-phenylindole (DAPI). The percentage of sporulated cells was determined by microscopy<sup>10</sup>.

### DNA-end resection assay

Cultures of *sae2 $\Delta$  cdc28-as1 GAL1::HO* strain transformed with wild-type *SAE2*, *sae2-S267A*, *sae2-S267E* or empty vector were grown to mid-exponential phase in raffinose. Samples were taken at indicated times after inducing HO by the addition of galactose. DNA was isolated, of which 1 mg was blotted in neutral and denaturing conditions with a dot-blot manifold as described previously<sup>23</sup>, then hybridized with radioactively labelled probes against the *MAT* locus, 5 kb downstream of the *MAT* locus or *LEU2* locus. Signals were quantified with a FLA-5000 instrument (Fuji) and values obtained in neutral conditions were normalized to those obtained under denaturing conditions (see Supplementary Fig. 3a). When indicated, 2 h before the addition of galactose, the culture was split in two and dimethylsulphoxide or Cdc28-as1 inhibitor 1NM-PP1 (5  $\mu$ M final concentration; Calbiochem) was added.

### Rad52 and Mre11 foci analyses

Mre11-YFP Rad52-RFP *sae2 $\Delta$*  strain transformed with *SAE2*, *sae2-S267A*, *sae2-S267E* or empty vector was irradiated (30 Gy) with a Faxitron (Faxitron X-ray Corporation). Samples were taken, fixed by the addition of 0.1 volume of formaldehyde, washed three times with PBS, sonicated for 10 s and mixed 1:1 with DAPI-containing mounting medium (Vector Laboratories Inc.). Microscopy was with a DeltaVision microscope (Applied Precision). A minimum of 50 G1 (unbudded) and 50 S/G2 (budded) cells were counted at each time point and for each sample.

### Survival of irradiation

*sae2 $\Delta$*  mutants transformed with wild-type *SAE2*, *sae2-S267A*, *sae2-S267E* or an empty vector were grown asynchronously or were arrested with  $\alpha$ -factor (G1) or nocodazole (G2); they were then irradiated with 300 Gy (Faxitron), kept for 6 h in the same cell-cycle stage and then plated. Colonies arising were normalized with respect to non-irradiated samples and plotted.

### NHEJ assays

A pRS416 vector restricted with *Xho* I, *Sac* I or *Sma* I was transformed into cells harbouring various *sae2* mutations. The number of colonies formed after 3 days was normalized with the number of colonies obtained in a parallel transformation with a circular pRS416 plasmid. Plasmids from 50 independent clones of each strain transformed with a *Xho* I-restricted plasmid as described previously were isolated and sequenced.

## References

1. Shrivastav M, De Haro LP, Nickoloff JA. Regulation of DNA double-strand break repair pathway choice. *Cell Res.* 2008; 18:134–147. [PubMed: 18157161]
2. Aylon Y, Liefshitz B, Kupiec M. The CDK regulates repair of double-strand breaks by homologous recombination during the cell cycle. *EMBO J.* 2004; 23:4868–4875. [PubMed: 15549137]
3. Caspari T, Murray JM, Carr AM. Cdc2-cyclin B kinase activity links Crb2 and Rqh1-topoisomerase III. *Genes Dev.* 2002; 16:1195–1208. [PubMed: 12023299]
4. Hinz JM, Yamada NA, Salazar EP, Tebbs RS, Thompson LH. Influence of double-strand-break repair pathways on radiosensitivity throughout the cell cycle in CHO cells. *DNA Repair (Amst.)*. 2005; 4:782–792. [PubMed: 15951249]
5. Ira G, et al. DNA end resection, homologous recombination and DNA damage checkpoint activation require CDK1. *Nature.* 2004; 431:1011–1017. [PubMed: 15496928]
6. Karathanasis E, Wilson TE. Enhancement of *Saccharomyces cerevisiae* end-joining efficiency by cell growth stage but not by impairment of recombination. *Genetics.* 2002; 161:1015–1027. [PubMed: 12136007]
7. Esashi F, et al. CDK-dependent phosphorylation of *BRCA2* as a regulatory mechanism for recombinational repair. *Nature.* 2005; 434:598–604. [PubMed: 15800615]
8. Aylon Y, Kupiec M. DSB repair: the yeast paradigm. *DNA Repair (Amst.)*. 2004; 3:797–815. [PubMed: 15279765]
9. Clerici M, Mantiero D, Lucchini G, Longhese MP. The *Saccharomyces cerevisiae* Sae2 protein promotes resection and bridging of double strand break ends. *J. Biol. Chem.* 2005; 280:38631–38638. [PubMed: 16162495]
10. McKee AH, Kleckner N. A general method for identifying recessive diploid-specific mutations in *Saccharomyces cerevisiae*, its application to the isolation of mutants blocked at intermediate stages of meiotic prophase and characterization of a new gene *SAE2*. *Genetics.* 1997; 146:797–816. [PubMed: 9215888]
11. Neale MJ, Pan J, Keeney S. Endonucleolytic processing of covalent protein-linked DNA double-strand breaks. *Nature.* 2005; 436:1053–1057. [PubMed: 16107854]
12. Prinz S, Amon A, Klein F. Isolation of *COM1*, a new gene required to complete meiotic double-strand break-induced recombination in *Saccharomyces cerevisiae*. *Genetics.* 1997; 146:781–795. [PubMed: 9215887]
13. Lengsfeld BM, Rattray AJ, Bhaskara V, Ghirlando R, Paull TT. Sae2 is an endonuclease that processes hairpin DNA cooperatively with the Mre11/Rad50/Xrs2 complex. *Mol. Cell.* 2007; 28:638–651. [PubMed: 18042458]
14. Baroni E, Viscardi V, Cartagena-Lirola H, Lucchini G, Longhese MP. The functions of budding yeast Sae2 in the DNA damage response require Mec1- and Tel1-dependent phosphorylation. *Mol. Cell. Biol.* 2004; 24:4151–4165. [PubMed: 15121837]
15. Mendenhall MD, Hodge AE. Regulation of Cdc28 cyclin-dependent protein kinase activity during the cell cycle of the yeast *Saccharomyces cerevisiae*. *Microbiol. Mol. Biol. Rev.* 1998; 62:1191–1243. [PubMed: 9841670]
16. Penkner A, et al. A conserved function for a *Caenorhabditis elegans* Com1/Sae2/CtIP protein homolog in meiotic recombination. *EMBO J.* 2007; 26:5071–5082. [PubMed: 18007596]
17. Sartori AA, et al. Human CtIP promotes DNA end resection. *Nature.* 2007; 450:509–514. [PubMed: 17965729]
18. Uanschou C, et al. A novel plant gene essential for meiosis is related to the human CtIP and the yeast *COM1/SAE2* gene. *EMBO J.* 2007; 26:5061–5070. [PubMed: 18007598]
19. Pommier Y. Topoisomerase I inhibitors: camptothecins and beyond. *Nature Rev. Cancer.* 2006; 6:789–802. [PubMed: 16990856]
20. Chen J, Saha P, Kornbluth S, Dynlacht BD, Dutta A. Cyclin-binding motifs are essential for the function of p21<sup>CIP1</sup>. *Mol. Cell. Biol.* 1996; 16:4673–4682. [PubMed: 8756624]
21. Lobachev KS, Gordenin DA, Resnick MA. The Mre11 complex is required for repair of hairpin-capped double-strand breaks and prevention of chromosome rearrangements. *Cell.* 2002; 108:183–193. [PubMed: 11832209]

22. Sugawara N, Haber JE. Repair of DNA double strand breaks: *in vivo* biochemistry. *Methods Enzymol.* 2006; 408:416–429. [PubMed: 16793384]
23. Bishop AC, et al. A chemical switch for inhibitor-sensitive alleles of any protein kinase. *Nature.* 2000; 407:395–401. [PubMed: 11014197]
24. Lazzaro F, et al. Histone methyltransferase Dot1 and Rad9 inhibit single-stranded DNA accumulation at DSBs and uncapped telomeres. *EMBO J.* 2008; 27:1502–1512. [PubMed: 18418382]
25. Lisby M, Barlow JH, Burgess RC, Rothstein R. Choreography of the DNA damage response: spatiotemporal relationships among checkpoint and repair proteins. *Cell.* 2004; 118:699–713. [PubMed: 15369670]
26. Rattray AJ, McGill CB, Shafer BK, Strathern JN. Fidelity of mitotic double-strand-break repair in *Saccharomyces cerevisiae*: a role for *SAE2/COM1*. *Genetics.* 2001; 158:109–122. [PubMed: 11333222]
27. Cortes-Ledesma F, Aguilera A. Double-strand breaks arising by replication through a nick are repaired by cohesin-dependent sister-chromatid exchange. *EMBO Rep.* 2006; 7:919–926. [PubMed: 16888651]
28. Boulton SJ, Jackson SP. *Saccharomyces cerevisiae* Ku70 potentiates illegitimate DNA double-strand break repair and serves as a barrier to error-prone DNA repair pathways. *EMBO J.* 1996; 15:5093–5103. [PubMed: 8890183]
29. Lee K, Lee SE. *Saccharomyces cerevisiae* Sae2- and Tel1-dependent single-strand DNA formation at DNA break promotes microhomology-mediated end joining. *Genetics.* 2007; 176:2003–2014. [PubMed: 17565964]
30. Limbo O, et al. Ctp1 is a cell-cycle-regulated protein that functions with Mre11 complex to control double-strand break repair by homologous recombination. *Mol. Cell.* 2007; 28:134–146. [PubMed: 17936710]
31. Puig O, et al. The tandem affinity purification (TAP) method: a general procedure of protein complex purification. *Methods.* 2001; 24:218–229. [PubMed: 11403571]



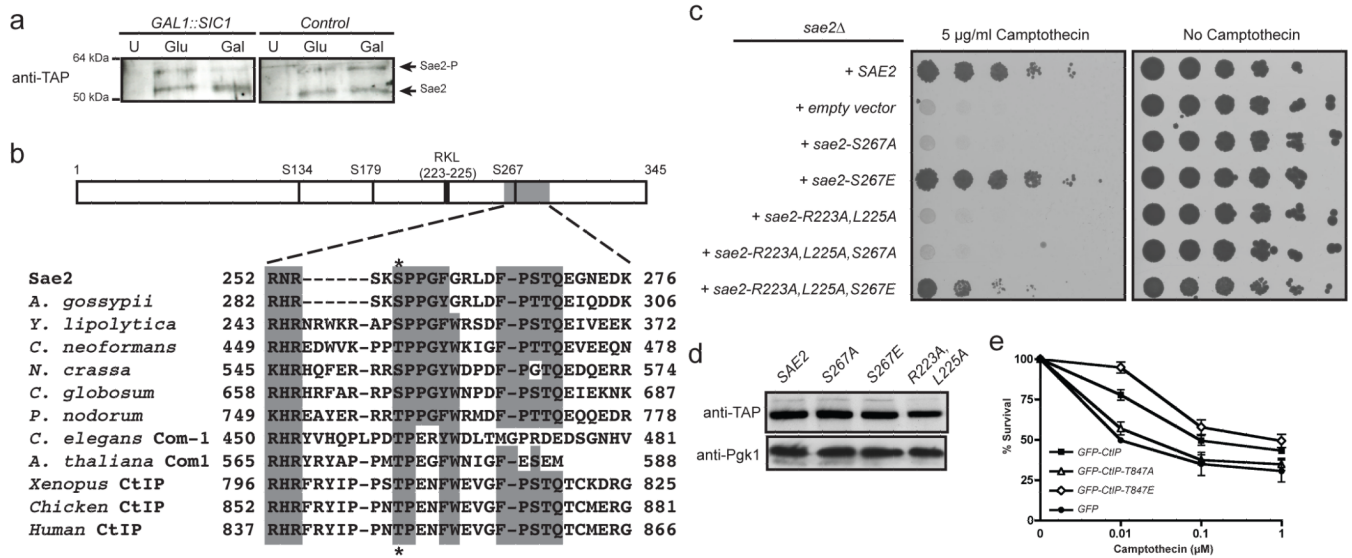


**Figure 1. Ser 267 mutation impairs Sae2 function**

**a**, Left: TAP-tagged Sae2 was purified from cells expressing galactose-inducible *SIC1* (Gal) or not expressing *SIC1* (Glc). U, control untagged strain. Right: as above, but the strain lacked galactose-inducible *SIC1*. **b**, Sae2 diagram and homology to orthologues (see Methods for full alignment). *S. cerevisiae*, *Saccharomyces cerevisiae*, *A. gossypii*, *Ashbya gossypii*, *Y. lipolytica*, *Yarrowia lipolytica*; *C. neoformans*, *Cryptococcus neoformans*, *N. crassa*, *Neurospora crassa*; *C. globosum*, *Chaetomium globosum*, *P. nodorum*, *Phaeosphaeria nodorum*; *C. elegans*, *Caenorhabditis elegans*; *A. thaliana*, *Arabidopsis thaliana*; *Xenopus*, *Xenopus laevis*; chicken, *Gallus gallus*; human, *Homo sapiens*. **c**, Fivefold serial dilutions of *sae2Δ* cultures containing the indicated *SAE2* genes plated on medium lacking or containing camptothecin (5 μg ml<sup>-1</sup>). **d**, Extracts of cells harbouring TAP-tagged Sae2 variants were western immunoblotted as indicated. **e**, Survival of U2OS cells expressing GFP-CtIP fusions to 1 h treatments with the indicated doses of camptothecin. Error bars indicate s.d. ( $n = 2$ ).

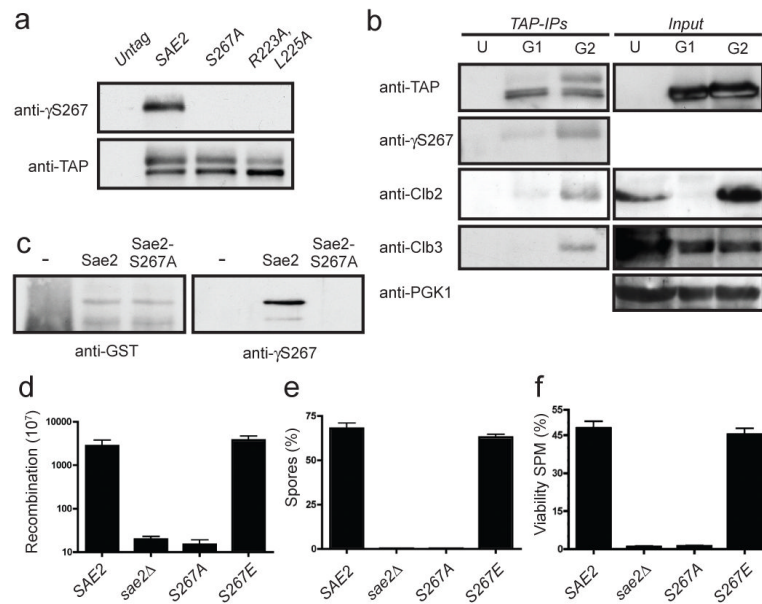


**Figure 2. Sae2 is phosphorylated by Cdc28 on Ser 267**

**a**, TAP-tagged Sae2 derivatives were immunoprecipitated and detected as indicated. **b**, TAP-tagged Sae2 was purified from G1 or G2 arrested cultures. U, G2 arrested untagged control cells. Immunoprecipitated samples and inputs (5%) were immunoblotted as indicated. **c**, Glutathione *S*-transferase (GST)-fused Sae2 and Sae2-S267A were purified, incubated with recombinant Cdk2/Cyclin A and ATP, resolved by 10% SDS-PAGE and immunoblotted as indicated. **d**, Recombination frequencies of strains in a hairpin-containing recombination system<sup>22</sup>. **e**, Spores after 24 h in sporulation medium. **f**, Spore viability 24 h after the addition of sporulation medium (SPM)<sup>10</sup>. Error bars in **d-f** represent s.d. ( $n = 2$ ).

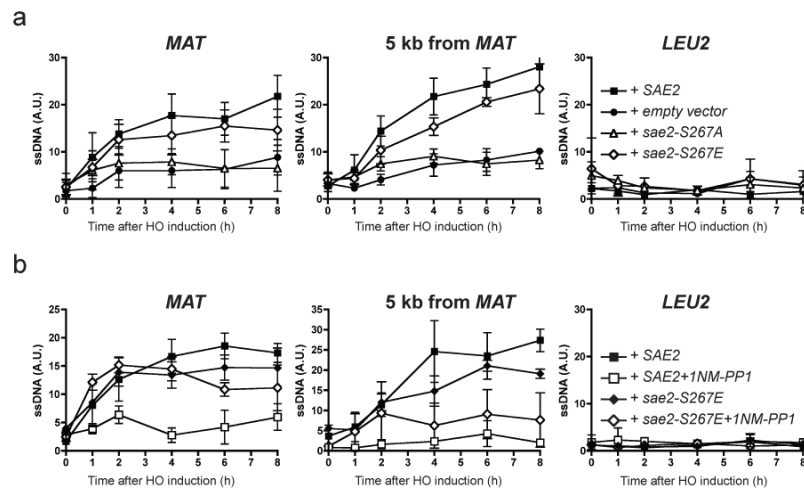


**Figure 3. DNA-end resection is controlled by Sae2**

**a**, Resection-mediated ssDNA formation at an HO DSB in wild-type *SAE2* (filled squares), *sae2-S267A* (open triangle), *sae2-S267E* (open diamonds) or empty vector (solid circles) at indicated times after HO induction at the *MAT* locus (left), 5 kb downstream of *MAT* (centre) or *LEU2* locus (right). **b**, Wild-type *SAE2* (squares) or *sae2-S267E* (diamonds) strains containing Cdc28-as1 were grown as in **a** but in the presence of dimethylsulphoxide (filled symbols) or 1NM-PP1 (open symbols). Results are shown as means  $\pm$  s.d. ( $n = 5$ ).

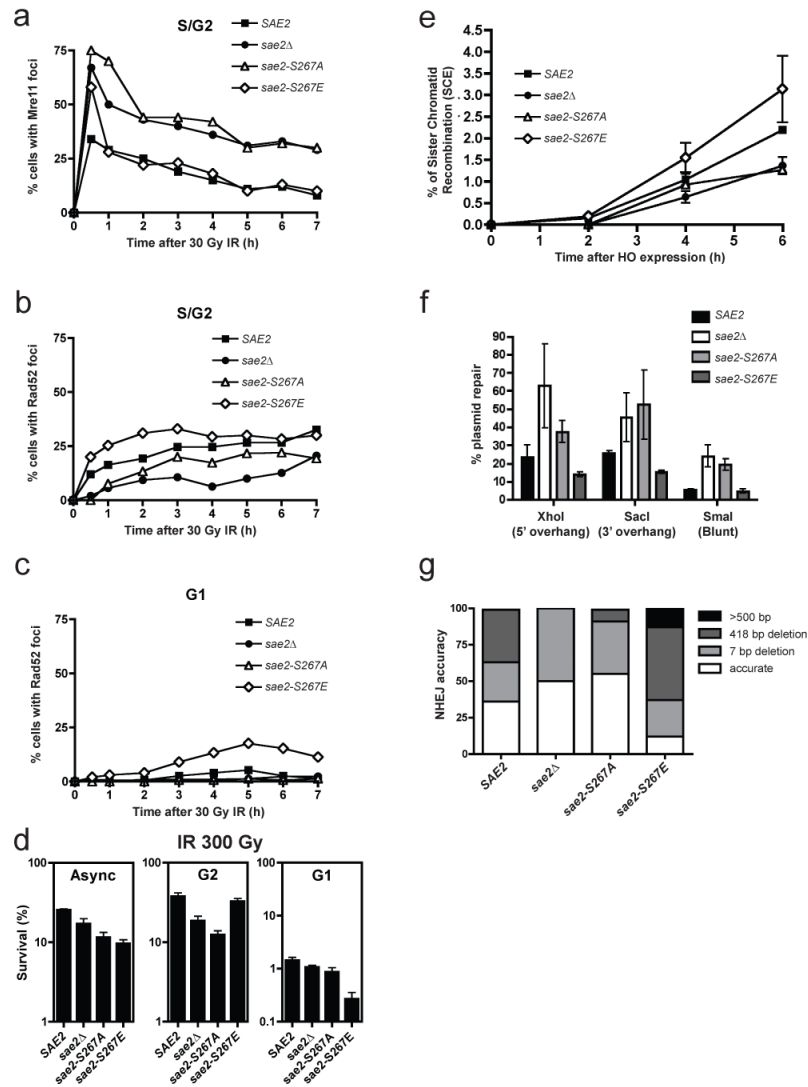


**Figure 4. Sae2 mutations affect Mre11 and Rad52 dynamics, and DSB repair**

**a, b**, Percentages of S/G2 cells containing Mre11 (**a**) or Rad52 (**b**) foci. **c**, Percentage of G1 cells containing a Rad52 focus. **d**, Survival of *sae2Δ* mutants containing wild-type *SAE2*, *sae2-S267A*, *sae2-S267E* or empty vector grown asynchronously (Async) or arrested in G1 or G2, after irradiation with 30 Gy. Error bars represent s.d. ( $n = 2$ ). **e**, Sister-chromatid recombination measured as described previously<sup>27</sup>. Standard deviations of two independent experiments are shown (see Supplementary Fig. 4 for details and representative blot). **f**, Plasmid cleaved by *Xho* I, *Sac* I or *Sma* I was transformed into strains and NHEJ efficiency was measured. Means and s.d. of three independent experiments are shown. **g**, Classes of plasmid rejoining products from 50 independent clones of each strain transformed with the *Xho* I-cut plasmid.